IL NUOVO CIMENTO **48 C** (2025) 53
DOI 10.1393/ncc/i2025-25053-x

Colloquia: IWM-EC 2024

Description of many-body correlations and clustering phenomena within a unified theoretical scheme

S. Burrello([1]), M. Colonna([1]), R. Wang([2]) and F. Matera([3])

([1]) *INFN, Laboratori Nazionali del Sud - I-95123 Catania, Italy*
([2]) *Istituto Nazionale di Fisica Nucleare (INFN), Sezione di Catania - I-95123 Catania, Italy*
([3]) *Dipartimento di Fisica e Astronomia, Università degli Studi di Firenze*
I-50019 Sesto Fiorentino, Firenze, Italy

received 26 November 2024

Summary. — Nuclear matter at subsaturation densities is expected to be inhomogeneous due to the emergence of many-body correlations, which are crucial for constructing a reliable equation of state. Specifically, large-scale correlations are responsible for fragmentation processes, experimentally observed in heavy-ion collisions at intermediate energies as the result of mechanical (spinodal) instabilities driven by the mean field, in connection to the occurrence of a liquid-gas phase transition. On the other hand, even at lower densities, owing to residual few-body correlations, light clusters like deuterons and strongly bound α particles also form but dissolve with increasing density due to the Pauli principle. Phenomenological models that make use of energy density functionals offer a way to include these clusters as additional degrees of freedom, yet a consistent description of both light clusters and heavy fragment formation through spinodal instabilities is still lacking. In this work, we propose a novel approach to incorporate in-medium modified clusters within a non-relativistic kinetic framework, unifying the description of clustering phenomena and heavy fragment formation at low densities.

1. – Introduction

The theoretical understanding of the properties of nuclear systems as a function of mass number, isospin asymmetry, excitation energy, or temperature requires addressing various many-body correlations and clustering phenomena. For instance, large-scale correlations may arise due to spinodal instabilities related to the liquid-gas phase transition, which is associated with the multifragmentation processes observed experimentally in heavy-ion collisions (HICs) at intermediate energies [1]. These reactions provide a unique tool to create transient states of nuclear matter (NM), possibly locally equilibrated, under conditions far from saturation in terrestrial laboratories, offering valuable insights into the NM equation of state (EOS) [2], in connection with astrophysical observations [3, 4].

On the other hand, few-body correlations induced by short-range nucleon-nucleon interactions are responsible for the formation of bound states of nucleons, as the system can minimize its energy at low densities by forming light clusters such as deuterons or α particles [5]. However, despite recent progress [6-9], a consistent description of the concurrent emergence of light clusters and heavier fragments remains challenging, particularly in dynamical studies. Phenomenological models utilizing energy density functionals (EDFs) provide a reliable avenue, at least from a thermodynamic perspective, as they incorporate clusters as explicit degrees of freedom (DOF), describing dilute NM as a mixture of nucleons and nuclei [5, 10, 11].

However, light clusters should dissolve at high densities due to the so-called Mott effect, primarily driven by Pauli blocking [12]. Recent approaches, such as the generalized relativistic density functional (gRDF) model, address this phenomenon assuming the medium modifies the effective binding energy of a cluster through a mass-shift [5]. The latter can be determined microscopically, at least at low densities, by solving the in-medium many-body Schrödinger equation and then parameterized as a function of density, temperature, isospin asymmetry, and center of mass (c.m.) momentum [12, 13]. However, these parameterizations rely on heuristic extrapolations to predict cluster dissolution beyond the Mott density, defined as the density where the effective binding energy of a cluster with zero c.m. momentum vanishes. Beyond this point, bound clusters exist only if their c.m. momentum exceeds a critical value known as the Mott momentum [12]. Yet, few-body correlations in the continuum might persist, even though they are not accounted for in phenomenological EDF-based models like the gRDF. An extension of the gRDF model was then recently proposed in ref. [14] to effectively incorporate residual few-body short-range correlations (SRCs) at supra-saturation densities in established EOS models.

The aim of this work is to consider a more general kinetic framework to address the dynamics of NM in the heterogeneous dilute regime, incorporating light (bound) clusters and their in-medium effects. To this end, in sect. **2**, we review a novel approach first proposed in ref. [15], which we develop as a first attempt to provide a unified framework for both light and heavy cluster formation at low densities, when out-of-equilibrium processes, such as those occurring in nuclear reactions, are considered. In sect. **2**, we present both theoretical formalism and the results. Conclusions and outlooks are outlined in sect. **3**.

2. – Dynamics of dilute matter with light clusters as degrees of freedom

The need to study the dynamics of nuclear matter arises from the fact that, as already anticipated in the introduction, a relevant source of information on the EOS comes from investigating out-of-equilibrium processes. In particular, central HIC at Fermi/intermediate energies (in the range of beam energies $E/A \approx 30-300\,\mathrm{MeV/nucleon}$) allow for the exploration of low-density regions and moderate temperatures during the expansion phase subsequent the initial compression [16, 17], probing a similar region of the phase diagram as in astrophysical phenomena, such as core-collapse supernovae or binary neutron star mergers [18]. Dynamical processes are commonly modeled with transport theories, which however fail to consistently account for the description of light clusters, emerging from few-body correlations and mean-field (MF) instabilities, which lead to the formation of intermediate mass fragments through spinodal mechanism. In particular, in a recent work [8], a kinetic approach based on the Boltzmann equation for the distribution function in the phase-space was developed. In this model, the in-medium Mott effect is taken into account by introducing a cut-off for the production of light clusters in the collision integral, providing a reasonable description of the yields measured by the FOPI Collaboration [19], with mass number up to 4. Inspired by this work, we delve into this context and investigate the fragmentation dynamics of a low-density system at a given temperature, composed of nucleons and light clusters. Our focus is on understanding how light clusters, which mainly arise from few-body correlations in the compression phase, influence the MF evolution and the development of spinodal instabilities, occurring in the expansion stage and ultimately leading to the disassembly of the system into fragments of various sizes. For that purpose, a non-relativistic framewok will be adopted, which allows for a more easily carried out dynamical treatment. The corresponding theoretical formalism is detailed in the next section.

2˙1. *Theoretical formalism.* – Let us consider a system of nucleons —neutrons (n) and protons (p)— and one light cluster species (deuterons (d), for the sake of illustration), all in thermodynamic equilibrium at temperature T. The total baryon density, $\rho_b = \sum_j \rho_j A_j$, is defined using the densities ρ_j and mass numbers A_j of the constituents ($j = n, p, d$). The phase-space distribution functions f_j are given by

$$f_j\left(\epsilon_j\right) = \left[\exp\left(\frac{\epsilon_j - \mu_j^*}{T}\right) - (-1)^{A_j}\right]^{-1}, \tag{1}$$

where μ_j^* is the effective chemical potential and $\epsilon_j = \frac{p^2}{2m_j}$. Here, $m_j = A_j m - B_j$, with $m = 939\,\mathrm{MeV}$ being the bare nucleon mass, and B_j the binding energy (zero for free nucleons). The number density ρ_j for each species is given by

$$\rho_j = g_j \int_{\Lambda_j} \frac{\mathrm{d}\mathbf{p}}{(2\pi\hbar)^3} f_j, \tag{2}$$

where g_j is the spin-degeneracy, and Λ_j is a momentum cut-off (Mott momentum) introduced for clusters ($\Lambda_j = 0$ for $j = n, p$) to account for in-medium effects like Pauli-blocking [8, 12, 15]. The cut-off Λ_j generally depends on the densities and temperature, thus simulating a momentum-dependent binding energy-shift. We assume surviving clusters retain their vacuum mass regardless of the medium density. The effects related to mass shift and momentum cut-off, as well as continuum correlations at higher densities, are beyond the scope of this work and are therefore neglected.

The thermodynamic properties of the system are fully described by its thermodynamic potential. At finite temperature, the relevant quantity is the free-energy density, $\mathcal{F} = \mathcal{E} - T\mathcal{S}$, where $\mathcal{S}$ is the entropy density, and $\mathcal{E}$ is the energy density, comprising kinetic ($\mathcal{K}$) and potential ($\mathcal{U}$) components. Within EDF theory, $\mathcal{U}$ is derived from a density-dependent effective interaction.

Our goal is to explain the formation of heavy fragments due to volume instabilities and the presence of light clusters within a unified theoretical framework. To achieve this, we perform a linear response analysis of the collisionless (Vlasov) limit of the Boltzmann equation, considering the interaction between nucleonic and light-cluster DOF while including in-medium effects [15]. By applying a small perturbation δf_j to the initial distribution functions f_j, the linearized Vlasov equations become

$$\partial_t(\delta f_j) + \nabla_{\mathbf{r}}(\delta f_j) \cdot \nabla_{\mathbf{p}}\varepsilon_j - \nabla_{\mathbf{p}} f_j \cdot \nabla_{\mathbf{r}}(\delta\varepsilon_j) = 0, \tag{3}$$

where the single-particle energy ε_j is defined as

$$\varepsilon_j \equiv \frac{(2\pi\hbar)^3}{g_j}\frac{\delta\mathcal{E}}{\delta f_j(\mathbf{p})}. \tag{4}$$

For simplicity, we use a momentum-independent Skyrme-like effective interaction as in ref. [2], leading to the single-particle energy

$$\varepsilon_j = \epsilon_j + U_j + \tilde{\varepsilon}_j^{\lambda}, \tag{5}$$

where $U_j = \frac{\partial \mathcal{U}}{\partial \rho_j}$ is the MF potential, and the effective potential term

$$\tilde{\varepsilon}_j^{\lambda} = -\frac{\lambda_d + U_d}{1 + \Phi_\lambda^{dd}}\Phi_\lambda^{dj}, \tag{6}$$

with

$$\Phi_\lambda^{dj} = \alpha_d \sqrt{\lambda_d} f_d\left(\lambda_d\right)\frac{\partial \lambda_d}{\partial \rho_j}, \tag{7}$$

and $\alpha_d = g_d \frac{(2m_d)^{3/2}}{4\pi^2\hbar^3}$ arises froms the density-dependent kinetic energy cut-off $\lambda_d = \frac{\Lambda_d^2}{2m_d}$. Notably, using eq. (2), the fluctuation in density can be expressed as

$$\delta\rho_j(\mathbf{r},t) = g_j \int_{\Lambda_j} \frac{\mathrm{d}\mathbf{p}}{(2\pi\hbar)^3}\delta f_j - \delta_{jd}\sum_l \Phi_\lambda^{dl}\delta\rho_l, \tag{8}$$

where the Kronecker function δ_{jd} is used. The meaning of the second term in the right-hand side of the above equation is that the local density of light nuclei may vary, not just because of fluctuations in the distribution function, but also due to the impact of density fluctuations along their propagation on in-medium effects driven by the density-dependent cut-off. Dynamically, this would also suggest that the rate of cluster formation or dissolution is much faster than the rate of local baryon density changes. However, to better understand the influence of in-medium effects, the opposite scenario might also be considered in the calculations, where the cut-off momentum remains constant during the propagation of density fluctuations ($\Phi_\lambda^{dj} = 0$).

Equation (3) allows for plane-wave solutions where δf_j oscillates with a frequency ω and wave vector $\mathbf{k}$, represented as $\delta f_j \sim \sum_{\mathbf{k}} \delta f_j^{\mathbf{k}}\, e^{i(\mathbf{k}\cdot\mathbf{r}-\omega t)}$. Using the Landau procedure [20], this leads to a system of three coupled equations for neutrons, protons, and deuterons which can be compactly written as [15]

$$\delta\rho_j = -\chi_j \sum_l (F_0^{jl} + \tilde{F}_\lambda^{jl})\delta\rho_l - \delta_{jd}\sum_l \Phi_\lambda^{dl}\delta\rho_l, \tag{9}$$

where $\chi_j = \chi_j(\omega,\mathbf{k})$ is the Lindhard function with a momentum cut-off. The parameters are defined as

$$F_0^{jl} = N_j \frac{\partial U_j}{\partial \rho_l}, \qquad \tilde{F}_\lambda^{jl} = N_j \frac{\partial \tilde{\varepsilon}_j^{\lambda}}{\partial \rho_l}, \qquad j,l = n,p,d. \tag{10}$$

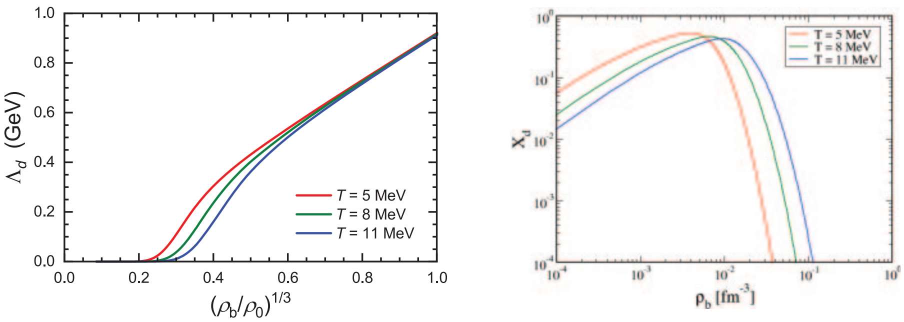

Fig. 1. – Left panel: Mott momentum of deuteron $\Lambda_d = \sqrt{2m_d\lambda_d}$ obtained by eq. (11) as a function of the cubic root of the (reduced) total baryon density, $(\rho_b/\rho_0)^{1/3}$ with $\rho_0 = 0.16$ fm^{-3}, for three temperature values. Readapted from ref. [15]. Right panel: ρ_b dependence of the deuteron mass fraction X_d for the same temperatures as in the left panel.

Here, $\tilde{F}^{jl}_{\lambda}$ are analogous to the Landau parameters F^{jl}_0, and N_j represents the thermally averaged level density, considering the momentum cut-off.

2·2. *Results.* – In this section we show the results obtained in the simplest case of symmetric nuclear matter (SNM) with deuterons as the only additional DOF. Indeed, although at low temperatures both quantum statistical (QS) and relativistic MF (RMF) calculations predict a dominance of α particles, in SNM at $T \gtrsim 5$ MeV (the range of interest here), the leading role is played by two-body correlations [15]. To model in-medium effects, we use the microscopic results from ref. [12] and define the kinetic energy cut-off as

$$\lambda_d(\rho_b, T) = \beta_d\, \rho_b^{\gamma_d} \left[1 + \tanh\left(1 - \xi_d \frac{\rho_d^{\mathrm{Mott}}(T)}{\rho_b}\right)\right], \tag{11}$$

where $\beta_d = 440\,\mathrm{MeV\ fm}^2$, $\xi_d = 2$, and $\gamma_d = 2/3$. This expression assumes a power-law dependence on baryon density, smoothed near the Mott density ρ_d^{Mott} to prevent discontinuities in the density derivatives of the cut-off. It also incorporates the temperature dependence of ρ_d^{Mott} as described in ref. [13]. The adopted deuteron Mott momentum parameterization, as plotted in fig. 1 (left panel) as a function of the total baryon density, was chosen in order to obtain, under chemical equilibrium conditions, a total baryon density behavior for the deuteron mass fraction $X_d = A_d\rho_d/\rho_b$, as shown in fig. 1 (right panel), which closely matches trends from QS or RMF calculations in ref. [5], in the region of temperatures of our interest. However, it is worthwhile to notice that the chemical equilibrium may actually not be achieved during the expansion phase of a nuclear reaction and can be relaxed in our calculations without affecting the results. These conditions represent indeed only the starting point of the dynamical treatment, which is presented hereafter.

The results are obtained by solving the homogeneous system given by eq. (9). In such a way, the dispersion relation, connecting the frequency ω to the wave number k, is correspondingly extracted. In particular, we are interested to the spinodal region, where the frequency becomes imaginary and the density fluctuations are amplified as a function of time, eventually leading to the disassembly of the system into pieces of various sizes. The onset of spinodal instabilities is identified by setting the determinant of the matrix in eq. (9) to zero for $\omega = 0$ ($\chi_q = \chi_d = 1$) [1,21]. The main panel of fig. 2 shows the spinodal

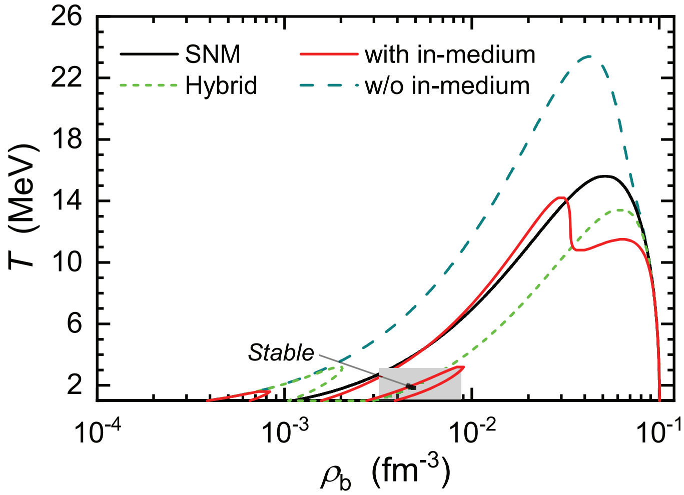

Fig. 2. – Spinodal boundary in the (ρ_b, T)-plane for three scenarios: 1) pure nucleonic matter (SNM, black); 2) nuclear matter with deuterons, including in-medium effects along the dynamics (red); 3) nuclear matter with deuterons, neglecting in-medium effects along the dynamics ($\Phi_\lambda^{dj} = 0$, cyan). A "hybrid" case is also shown (green, see text for details). Readapted from ref. [15].

border in the (ρ_b, T)-plane, with the red line representing the case where the local density dependence of the cut-off is considered. This curve is compared with the cyan line, where the density dependence of the cut-off is neglected ($\Phi_\lambda^{dj} = \tilde{F}_\lambda^{jl} = 0$), reducing the spinodal border condition to

$$(1 + F_0)\left(1 + F_0^{dd}\right) - 2F_0^{qd}F_0^{dq} = 0, \tag{12}$$

where $q = n$ or p, and $F_0 = F_0^{nn} + F_0^{np}$, leading to the standard pure nucleonic matter relation $(1 + F_0) = 0$ (black line) when $N_d \to 0$, *i.e.*, without light clusters. For illustration, the green line shows a "hybrid" case where the density dependence of the cut-off is ignored only in the single-particle energies ($\tilde{F}_\lambda^{jl} = 0$), while $\Phi_\lambda^{dj} \neq 0$ is retained in eq. (9). Generally speaking, including light clusters as explicit DOF significantly affects the extent of the spinodal region. Neglecting in-medium effects ($\Phi_\lambda^{dj} = 0$) would expand the instability region due to the stronger attraction from the deuteron MF potential, affecting F_0^{dd}. Conversely, in the hybrid case, the unstable region shrinks because in-medium effects raise the deuteron kinetic energy. Notably, when fully considering in-medium effects (red line), the spinodal border of the composite system aligns more closely with pure nucleonic matter (black line). The interplay between deuteron attraction and in-medium effects also creates small, isolated instability regions at low temperatures in both the hybrid and full cases (below 0.002 fm^{-3}). In the full calculations, another re-entry into the spinodal instability region is observed at higher densities, echoing recent findings on the emergence of a meta-stable region [22].

Inside the spinodal region, the frequency turns out to be purely imaginary. Then ω quantifies the growth rate of the unstable modes, which, plotted against the wave number k in fig. 3 for the same cases as in fig. 2, varies with density and temperature. The exhibited behavior causes the growth rate to peak at a specific k, indicating that the system favors the growth of density fluctuations at that particular wave number. The panels suggest that when in-medium effects are included in the dynamics, the maximum growth

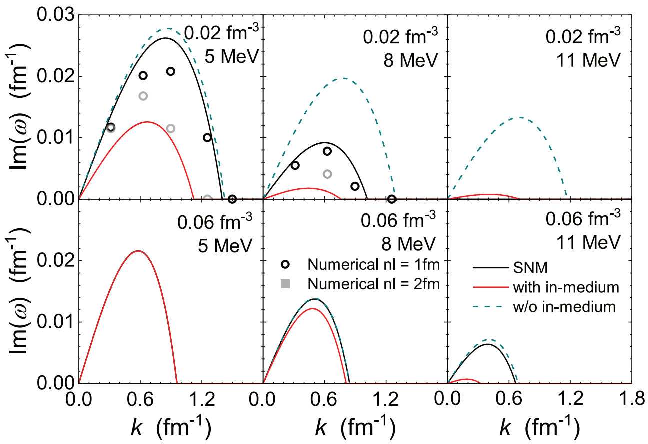

Fig. 3. – The growth rate of the instability, $\mathrm{Im}(\omega)$, is shown as a function of the wave number k for the same cases as in fig. 2, at various density and temperature values. The points represent preliminary results obtained by numerically solving the Vlasov equation for pure nucleonic matter, with two different sizes for the test-particle wave packets.

rate is reduced and shifted to lower k-values, slowing the instability growth and favoring different fragmentation modes. Conversely, neglecting in-medium effects would lead to the opposite behavior. It is also noteworthy that light clusters have a minimal impact on the growth of spinodal instabilities for densities above $\rho_0/3$ and at moderate temperatures. The direction of unstable modes within the space of density fluctuations is finally given by the ratio $(\delta\rho_S/\delta\rho_d)$, where ρ_S represents the total isoscalar nucleonic density. In fig. 4, the relative ratio $(\delta\rho_S/\delta\rho_d)\,/\,(\rho_S/\rho_d)$ is plotted as a function of ρ_b within the spinodal region, considering the two different approaches to in-medium effects discussed earlier. Positive values indicate that nucleons and deuterons fluctuate in phase, while negative values suggest they fluctuate out of phase. One observes that when in-medium effects are ignored, light clusters move in phase with nucleons, promoting instability growth and potentially contributing to the formation of larger fragments. In contrast, when in-medium effects are included, deuterons fluctuate out of phase with nucleons,

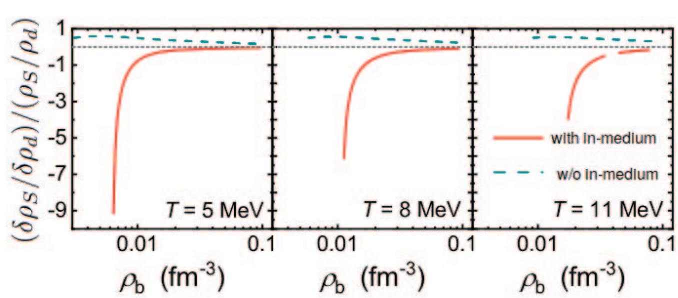

Fig. 4. – The relative ratio $(\delta\rho_S/\delta\rho_d)\,/\,(\rho_S/\rho_d)$ (see text) as a function of the total baryon density ρ_b for nuclear matter with deuterons, neglecting (cyan) or including (red) in-medium effects in the dynamics, for three temperature values. Lines are drawn only for the density values lying inside the spinodal region.

migrating to lower-density regions as nucleon density fluctuations grow and fragments form. This in-medium effect definitely acts as a "distillation" mechanism, leading to the separate emission of deuterons and potentially increasing their yield in mean-field–based simulations of HICs at intermediate energies, matching recent experimental findings concerning fragmentation dynamics [23].

3. – Summary, outlooks and conclusions

Summarizing, using a linearized Vlasov approach, in this work we have investigated the occurrence of spinodal instabilities in the dynamics of dilute NM, incorporating light-cluster DOF. Our results demonstrate that the presence of light clusters, particularly the in-medium (Mott) effects on their propagation, significantly influences the characteristics of the unstable modes that drive the disassembly of the system underlying the multi-fragmentation processes experimentally observed. When in-medium effects are ignored, light clusters move in phase with nucleons, aiding in fragment formation. However, local in-medium effects trigger a "distillation" mechanism, causing clusters to migrate towards lower density regions. This process slows down the growth of instabilities and affects the dominant fragmentation modes. These findings highlight the importance of accurately including light-cluster DOF and in-medium effects in the description of dilute nuclear systems, with critical implications for understanding HICs and astrophysical phenomena in low-density and moderate-temperature environments.

Several potential developments and future directions are envisaged for this work. Firstly, our results assume that nucleons bound in deuterons experience the same MF potential as free nucleons. However, recent EOS calculations for astrophysical applications conducted within the relativistic RMF approach [11, 14], suggest that other scenarios could be more appropriate due to the screening of interactions in the medium, affecting the chemical equilibrium constants. Additionally, beyond the linearized Vlasov approach discussed in this paper, a hydrodynamical perspective offers an alternative method to explore spinodal instability [24]. The relationship between these two approaches, particularly with the non-standard choice of a density-dependent cut-off in the momentum integrals, is currently under investigation and will be addressed in a forthcoming paper.

It would also be valuable to extend the current analysis to include α-clusters and, in the case of asymmetric nuclear matter (NM), other light cluster species. This could involve exploring different parameterizations for the effective interaction and the density-temperature dependence of the momentum cut-off.

More generally, to obtain a realistic description and allow for comparison with experimental data, one must move beyond the current quasi-analytical approach and perform fully numerical calculations by solving the Vlasov equation, for example, using the test-particle method. In the left and center top panels of fig. 3, the numerically obtained growth rates for several wave vectors are compared with those previously derived from the linearized Vlasov equations for pure nucleonic matter at a chosen density value of $\rho_b = 0.02\,\mathrm{fm}^{-3}$ and two temperatures ($T = 5$ and $8\,\mathrm{MeV}$). It is observed that the finite size of the (triangular) profiles assumed for the test particles in coordinate space generally reduces the instability growth rate. However, the numerical results converge to the quasi-analytical solutions as nl, which corresponds to the range of the test-particle packet, approaches zero. Work is ongoing to include light clusters and in-medium effects within this numerical framework, with the ultimate goal of providing a consistent description of the different mechanisms responsible for fragment formation in HICs at intermediate energies.

REFERENCES

[1] Chomaz P., Colonna M. and Randrup J., *Phys. Rep.*, **389** (2004) 263.
[2] Baran V., Colonna M., Greco V. and Di Toro M., *Phys. Rep.*, **410** (2005) 335.
[3] Huth S. *et al.*, *Nature*, **606** (2022) 276.
[4] Tsang C. Y., Tsang M. B., Lynch W. G., Kumar R. and Horowitz C. J., *Nat. Astron.*, **8** (2024) 328.
[5] Typel S., Röpke G., Klähn T., Blaschke D. and Wolter H. H., *Phys. Rev. C*, **81** (2010) 015803.
[6] Danielewicz P. and Bertsch G. F., *Nucl. Phys. A*, **533** (1991) 712.
[7] Ono A., *Prog. Part. Nucl. Phys.*, **105** (2019) 139.
[8] Wang R., Ma Y.-G., Chen L.-W., Ko C. M., Sun K.-J. and Zhang Z., *Phys. Rev. C*, **108** (2023) L031601.
[9] Cheng H.-G. and Feng Z.-Q., *Phys. Rev. C*, **109** (2024) L021602.
[10] Burrello S., Gulminelli F., Aymard F., Colonna M. and Raduta A. R., *Phys. Rev. C*, **92** (2015) 055804.
[11] Pais H., Gulminelli F., Providência C. and Röpke G., *Phys. Rev. C*, **99** (2019) 055806.
[12] Röpke G., *Phys. Rev. C*, **92** (2015) 054001.
[13] Röpke G., *Nucl. Phys. A*, **867** (2011) 66.
[14] Burrello S. and Typel S., *Eur. Phys. J. A*, **58** (2022) 120.
[15] Wang R., Burrello S., Colonna M. and Matera F., *Phys. Rev. C*, **110** (2024) L031601.
[16] Colonna M., *Prog. Part. Nucl. Phys.*, **113** (2020) 103775.
[17] Sorensen A., Agarwal K., Brown K. W., Chajęcki Z., Danielewicz P., Drischler C., Gandolfi S., Holt J. W., Kaminski M., Ko C.-M. *et al.*, *Prog. Part. Nucl. Phys.*, **134** (2024) 104080.
[18] Most E. R., Motornenko A., Steinheimer J., Dexheimer V., Hanauske M., Rezzolla L. and Stoecker H., *Phys. Rev. D*, **107** (2023) 043034.
[19] Reisdorf W., Andronic A., Averbeck R., Benabderrahmane M., Hartmann O., Herrmann N., Hildenbrand K., Kang T., Kim Y., Kiš M., Koczoń P., Kress T., Leifels Y., Merschmeyer M., Piasecki K., Schüttauf A., Stockmeier M., Barret V., Basrak Z., Bastid N., Čaplar R., Crochet P., Dupieux P., Dželalija M., Fodor Z., Gasik P., Grishkin Y., Hong B., Kecskemeti J., Kirejczyk M., Korolija M., Kotte R., Lebedev A., Lopez X., Matulewicz T., Neubert W., Petrovici M., Rami F., Ryu M., Seres Z., Sikora B., Sim K., Simion V., Siwek-Wilczyńska K., Smolyankin V., Stoicea G., Tymiński Z., Wiśniewski K., Wohlfarth D., Xiao Z., Xu H., Yushmanov I. and Zhilin A., *Nucl. Phys. A*, **848** (2010) 366.
[20] Landau L., *Sov. Phys. JETP*, **8** (1959) 70.
[21] Burrello S., Colonna M. and Matera F., *Phys. Rev. C*, **89** (2014) 057604.
[22] Röpke G., Voskresensky D., Kryukov I. and Blaschke D., *Nucl. Phys. A*, **970** (2018) 224.
[23] Borderie B., Le Neindre N., Rivet M., Désesquelles P., Bonnet E., Bougault R., Chbihi A., Dell'Aquila D., Fable Q., Frankland J. *et al.*, *Phys. Lett. B*, **782** (2018) 291.
[24] Burrello S., Colonna M. and Matera F., *Phys. Rev. C*, **89** (2014) 057604.